UDC 621.039.673

HIGH FIELD TOKAMAKS AS COMPACT NEUTRON SOURCES

F.P. Orsitto[1], M. Romanelli[2], M. Vinay[3]

[1]*ENEA, Department Fusion and Nuclear Safety, Frascati, Italy*
[2]*Tokamak Energy Ltd., 173 Brook Drive, Milton Park, Oxon, OX14 4SD, United Kingdom*
[3]*Institute of Plasma Research, Gandinaghar, Gujarat, India*

Fusion reactor scaling laws can be used to define plasma parameters of high field compact tokamak for low fusion gain applications as it is the case of compact neutron sources. The attractive physics of the high field tokamaks explored on Alcator devices and FTU has demonstrated that tokamaks (at magnetic field $B \geq 7$ T) can be operated in L-mode with substantial increase of confinement. In particular the operation with pellets is attractive in this respect because it opens up the possibility of operating the machine in ohmic plasmas at very high density (plasma density $n_e \geq 1 \cdot 10^{20}$ m^{-3}) with improved confinement properties. The compact high field tokamaks are characterized by a fundamental ohmic confinement with possibly a low RF heating power because of the limited space available. This paper is dedicated to i) a summary of the physics of high field tokamaks as derived from the database of FT, FTU and Alcator devices (including Alcator-C-MOD); ii) a discussion of their confinement properties in scenarios operated with pellets; iii) the scaling laws for fusion reactors, which allow for the evaluation of the geometry and plasma parameters of compact high field ($B \geq 7$ T) tokamaks at aspect ratio $A \geq 2.5$ and at low aspect ratio ($A < 2$); iv) the technical feasibility of these neutron sources and their technology readiness level.

Key words: high field tokamaks, compact fusion neutron sources.

DOI: 10.21517/0202-3822-2021-44-2-47-56

ТОКАМАКИ С СИЛЬНЫМ ПОЛЕМ КАК КОМПАКТНЫЕ ИСТОЧНИКИ НЕЙТРОНОВ

Ф.П. Орситто[1], М. Романелли[2], М. Винай[3]

[1]*ENEA (Национальное агентство по новым технологиям, энергетике и устойчивому развитию экономики), Отделение безопасности термоядерной и ядерной энергетики, Фраскати, Италия*
[2]*ООО «Токамак Энерджи», 173 Brook Drive, Milton Park, Oxon, OX14 4SD, Великобритания*
[3]*Институт исследований плазмы, Гандинагар, Гуджарат, Индия*

Законы масштабирования термоядерного реактора могут быть использованы для определения параметров плазмы компактного токамака с сильным полем (ТСП), с низким отношением термоядерной мощности к затрачиваемой, как в случае компактных источников нейтронов. Привлекательная физика ТСП, исследованных на токамаках Alcator и FTU, показала, что токамаки (при магнитном поле $B \geq 7$ Тл) могут работать в L-режиме с значительным увеличением удержания. В частности, привлекательна инжекция пеллет, поскольку она открывает возможность работы токамака с омической плазмой, имеющей очень высокую плотность ($n_e \geq 1 \cdot 10^{20}$ м$^{-3}$) и обеспечивающей лучшее удержание. Компактные ТСП характеризуются тем, что в них в основном используется омическое удержание с небольшой добавкой радиочастотного нагрева из-за ограниченного пространства. В статье даётся обзор физики ТСП на основе данных, полученных на токамаках FT, FTU и ALCATOR (включая Alcator-C-MOD), обсуждается удержание плазмы в таких токамаках при инжекции пеллет, рассматриваются скейлинги для термоядерных реакторов, позволяющие оценить геометрические характеристики и параметры плазмы компактных ТСП ($B \geq 7$ Тл) при аспектных соотношениях $A \geq 2{,}5$ и при $A < 2$, обсуждается техническая осуществимость этих источников нейтронов и уровень их технологической готовности.

Ключевые слова: токамаки с сильным полем, компактные термоядерные источники нейтронов.

INTRODUCTION

Recently, advances in the area of superconducting magnet technologies have opened up the prospekt of operating tokamak-type fusion reactors at higher magnetic fields [1, 2]. However, experimental data available for tokamak plasmas at high fields (>6 T) are scarce. Advantages of high field operation for fusion based tokamaks are well known. At fusion relevant temperatures in the range of 10—20 keV, the fusion power scales as $P_{\text{fus}} = \beta^2 B^4 R^3 / A^2$, where B is the toroidal magnetic field on axis, R the major radius of the tokamak, the aspect ratio A — major radius/minor radius, β = kinetic pressure/magnetic pressure. Various high field based tokamak fusion reactors are proposed for this purpose, such as Ignitor [3], SPARC [1] and ARC [4]. Current experiments however operate at relatively lower magnetic fields (<5 T). Extensive data for studying the physics at high fields $B > 6$ T is only limited to a handful of tokamaks that are currently not in operation. There is also a need to create a dedicated database for high field tokamaks that will serve as a basis for the design of tokamaks operating at

high fields in the near future due to the advancement of magnetic technologies capable of operating at higher fields. Only five tokamaks have operated till date with fields higher that 6 T. These are the Alcator family — Alcator-A, Alcator-C, and Alcator-C-MOD [5—9], the Frascati Tokamak (FT) [10—12] and Frascati Tokamak Upgrade (FTU) [13, 14]. This paper will mainly focus on the experimental results from these high field tokamaks in the ohmic regime which will serve as the possible baseline operational scenario for the compact neutron source. Operation in the ohmic regime has the advantage over the standard ELMy H-mode due to the absence of ELMs (edge localized modes). Moreover the power threshold for entering into the H-mode (high confinement mode) P_{LH} scales with the toroidal magnetic field [15]: i.e. $P_{LH} \approx B^{4/5}$, and this means that higher power would be needed to get into H-mode. Experiments on Alcator-C-MOD showed that the scaling of the power threshold for entering the H-mode is approximately P_{LH}, MW = 0.044nBS where n is the line average electron density, S is the last close magnetic surface area [20]. More detailed investigations in Alcator-C-MOD (for magnetic fields $B \leq 5.4$ T) showed that there is a minimum power $P_{LH} \approx 1.5$ MW at a density close to $n = 1.5\ 10^{20}$ m^{-3} [21]. H-mode obtained at $B = 7.9$ T with lithium pellet injection is reported using ICRF H and He^3 minority heating. High field operation for spherical tokamaks (ST) is also considered in the present study [16—19]. The extrapolation of low field ST data to high fields is used for determining the scaling at higher fields. The paper is divided into five sections. i) will summarise briefly the experimental evidences from high field tokamaks having a large aspect ratio supporting the operation in the ohmic regime; ii) is dedicated to design criteria for a MCF (magnetic confinement fusion) neutron source to define the scaling laws for tokamak fusion reactor plasmas. The determination of the parameters of a high field tokamak as a fusion neutron source is carried out. The method used was presented at FUNFI3 conference [22]; iii) includes the determination of the parameters of an ST as a neutron source based on the confinement scaling laws of NSTX, START and MAST [19]; iv) is dedicated to the technology readiness level (TRLs) of tokamak sub-systems. Conclusion and perspectives for the future work are outlined in v). The results reported are based only on theoretical physics analysis, the engineering constraints (such as the shieldings which must be included in the design of tokamak devices) are not considered in the present analysis.

SUMMARY OF RELEVANT EXPERIMENTAL RESULTS FROM HIGH FIELD TOKAMAKS: ALCATOR-A, ALCATOR-C, C-MOD, FT AND FTU

A summary of ohmic based discharges from high field machines Alcator A-C, Alcator-C-MOD, FT, and FTU is reviewed here. Table 1 below shows the main physics parameters of the machines. While FT, FTU and Alcator-C are all circular limiter plasma machines, Alcator-C-MOD is the only divertor machine to operate at a field of more than 5 T. Operation at higher field allows operation at higher densities thus allowing operation at a higher Lawson confinement parameter.

T a b l e 1. **High field machine parameters**

Parameter	Alcator-A	Alcator-C	Alcator-C-MOD	FT	FTU
Major radius, m	0.54	0.58—0.71	0.68	0.83	0.935
Minor radius, m	0.10	0.10—0.17	0.21	0.20	0.305
Plasma current, MA	0.3	0.8	3.0	0.6	1.6
Magnetic field, T	9	13	9	10	8
Divertor/Limiter	Circular plasmas	Circular limiter plasmas	Divertor plasma	Circular plasmas	Circular limiter plasms
Heating					
ECRH					140 GHz, 0.5 MW
LHCD	2.45 GHz 100 kW	2.45 GHz, 70 kW and 4.6 GHz, 1.5 MW	4.6 GHz, 3 MW	2.45 GHz	8 GHz, 1 MW
ICRH		180 MHz, 500 kW	40—80 MHz, 8 MHz		433 MHz, 0.5 MW

Ohmic confinement and density limit in high field tokamaks. *Alcator-C tokamak.* Experiments performed on Alcator-C at densities $\leq 8\times10^{20}$ m^{-3}, plasma current $\leq$0.75 MA and magnetic fields $\leq$13 T [28] showed that the turbulent trapped electron modes (TEM) regime dominates at lower densities, in the linear ohmic confiment, where the Alcator scaling is valid, and ion temperature gradient (ITG) turbulence dominate at higher densities, leading to a saturation of the energy confinement time at high densities. Subsequent experiments with frozen deuterium pellets [30] showed that pellet fuelled plasmas do not show a saturation of the confinement time as seen in conventional gas puffing due to supression of the ITG regime, leading to an

increase in confinement time. Fig. 1 below has been adopted directly [30], shows the increase in the confinement time with pellets.

FTU Tokamak. High density experiments on FTU have been extensively performed using pellets with the repeatative pellet enhanced plasma (PEP) modes leading to improved confiment [29]. This is again due to the reduced ion transport accompanied with supression of sawtooth activity. Experiments were carried out at a magnetic field of 7.1 T and a plasma current of 0.8 MA, where the density was increased from 1.5×10^{20} to 7.0×10^{20} m^{-3} with a drastic increase in the neutron rate of 4×10^{12} n/s. Further optimization extended this regime to 8 T and 1.25 MA plasma current with multiple pellets. Record neutron rates were achieved for FTU up to 1.5×10^{13} n/s, High confinement factor $H_{97} \geq 1.1$ with respect to the ITER-97L scaling law was achieved with these parameters. The figures reported in this section are extracted from [13, 14]. The ohmic operation at high field in FT, FTU, Alcator-C and Alcator-C-MOD was characterized by the Alcator scaling (the FTU ohmic scaling law is presented here):

$$\tau_E, \text{ ms} = Kn_e(10^{20}\ \text{m}^{-3})q^{1.42\pm0.07},\ K = 7.1\pm0.6, \qquad (1)$$

where K is a dimensional numerical constant, q the cylindrical safety factor and τ_E is the confinement time, ms.

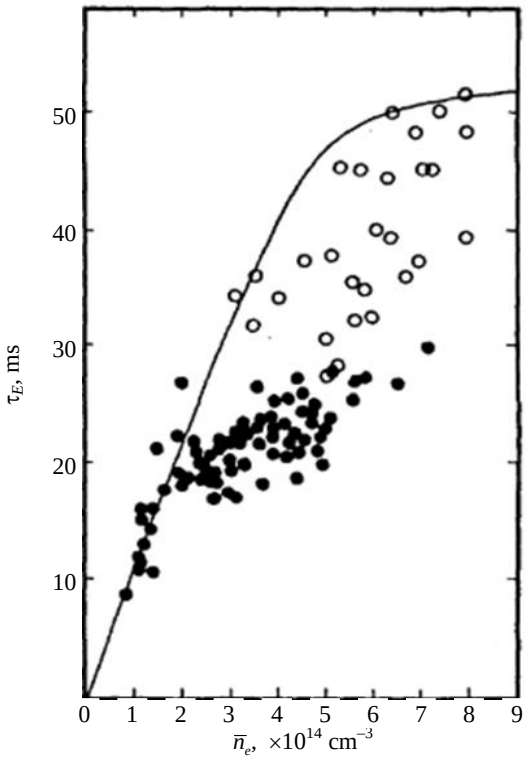

Fig. 1. Effect of pellets on the confinement time (adopted from [30]): • — gas-fueled; ○ — pellet-fueled

Fig. 2 shows a database of FTU where the confinement time vs the electron density is reported at various currents [1]. In Fig. 2, it is seen that the linear (vs density) ohmic confinement (LOC) regime holds up to a critical density, beyond which the SOC (saturated ohmic confinement) holds. The LOC regime is however seen to extend beyong the critical density with pellet operation, thus allowing for higher confinement times. Fig. 3 shows a comparision of the confinement time in FTU before and after pellet injection. There is good consistency of the confinement time with the L-mode scaling. There is almost a doubling of the confiment time as shown for the FTU pulse № 12 744 with the L-mode ITER-89P scaling law of confinement, in presence of pellets $\dfrac{\tau_{E_{\text{Pellet}}}}{\tau_{E_{\text{ITER-89P}}}} \sim 2$.

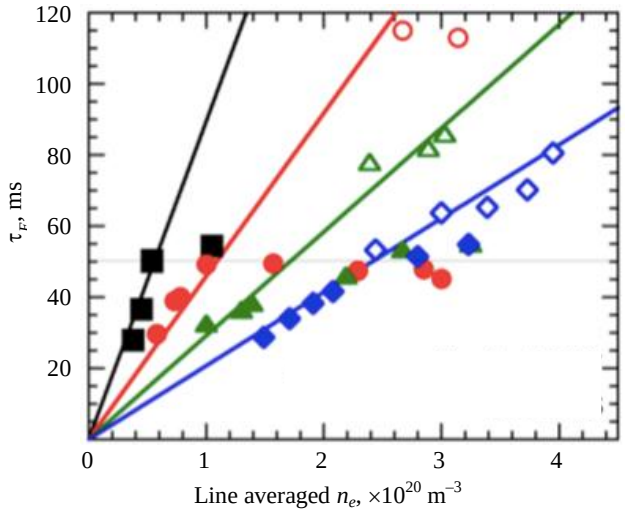

Fig. 2. FTU confinement time vs electron density at various plasma currents: ■ — 0.5; • — 0.8; ▲ — 1.1; ◆ — 1.4 MA. Open symbols correspond to pellet operations. The horizontal line is the value of the saturated ohmic confinement time on FTU. The plot shows that pellet operation recovers the linear scaling at high density [13, 14]. $\tau_{E\text{-linear}} = Kn_e(10^{20}\ \text{m}^{-3})q^{1.42\pm0.07}$, $K = 7.1\pm0.6$

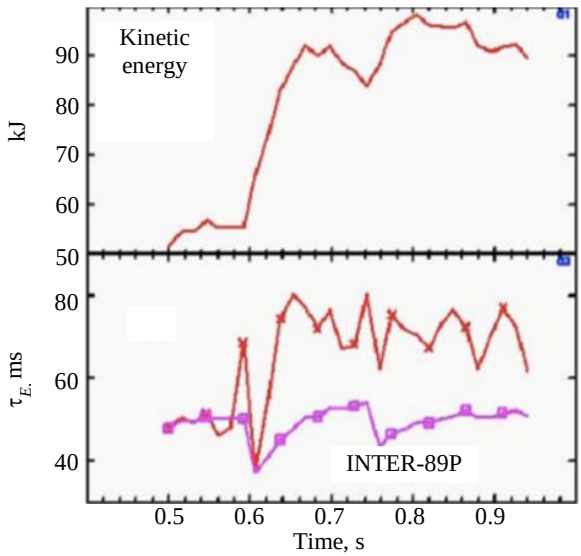

Fig. 3. Comparison between the ITER-89P L-mode confinement scaling law and confinement time measured with pellets, together with the increase of the plasma kinetic energy evolution are shown. Plasma parameters of FTU pulse № 12 744 are: $B_T = 6.88$ T, n_e (line average) $= 2\cdot10^{20}$ m^{-3}

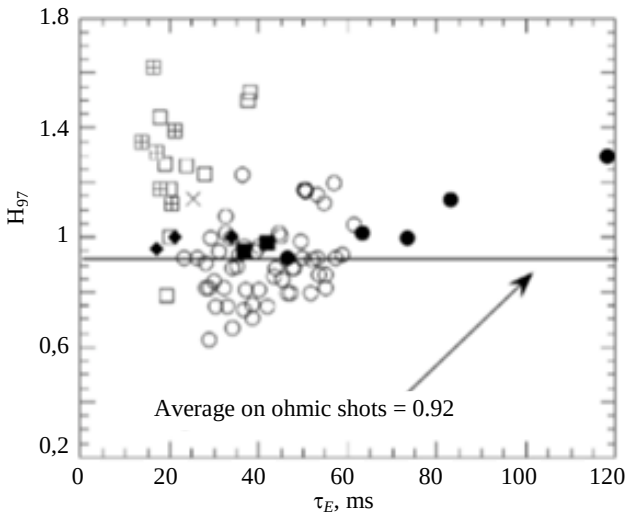

Fig. 4. FTU Database showing the H_{97} confinement improvement factor with respect to the L-mode confinement scaling law ITER-97P. $H_{97} \leq 1.3$ with pellet operation: ○ — OH; □ — LH —; (— LH + ECRH; × — ECRH; ◆ — IBW; ■ — RI; ● — pellet

Fig. 4 shows a plot of the confinement factor H_{97} of the FTU database with the ITER-97 L-mode scaling where $H_{97} = \tau_E$ measured/τ_E ITER-97 is the ratio of measured confinement time and that evaluated using the ITER L-mode scaling. The results indicate that a confinement factor of $H_{97} \approx 1.3$ can be obtained with pellet fuelled discharges.

Fig. 4 also includes data from discharges with ohmic heating and ohmic pellet operation, as well auxiliary radiofrequency (RF) heated discharges using Lower Hybrid (LH), electron cyclotron (ECRH), IBW (Ion Bernstein wave), and RI (improved highly radiating mode). In this context it can be noted that ohmic pellet operation reaches H_{97} values close to that obtained in ITB discharges where LH was combined with ECRH.

The Table 2 shows the detailed consistency of the parameters of the FTU pellet injected pulse № 12 744 (see also Fig. 2) with those obtained by the system code SPECTRE [26] using L-mode ITER-97P confinement scaling law: $H_{97} = 1.27$ is found by the system code to reproduce the FTU discharge parameters.

T a b l e 2. **Plasma parameters of the FTU pellet pulse № 12 744 with SPECTRE system code calculations using ITER-97P L-mode confinement scaling law**

Parameters	FTU 12 747	SPECTRE system code
H_{97}	1.23	1.25
R_0, m	0.9414	0.9407
A	3.35	3.35
I_p, MA	0.7931	0.7904
B_T, T	6.88	6.88
n_{line}, 10^{20} m^{-3}	2.71	2.64
n_{avg}, 10^{20} m^{-3}	—	1.32
$<T_e>$, keV	—	1.1
T_{e0}, keV	1.47	1.77
τ_E, ms	88.1	87.1
P_{OH}, MW	1.18	1.06
q_{95}	4.869	4.27
Z_{eff}	1.0	1.27
β_P	0.393	0.372
W_{therm}, kJ	107.3	103
V_{loop}, V	1.489	1.47
Neutron yield, s^{-1}	5.4×10^{12}	—

The parameters of the FTU pulse are included in the database international multi-tokamak confinement profile database http://tokamak-profiledb.ukaea.org.uk.

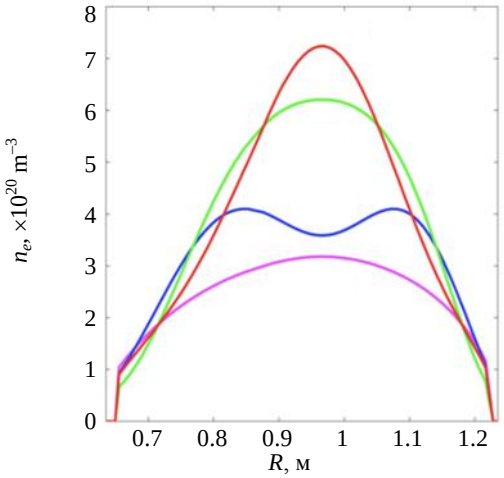

Fig. 5. Time evolution of the Abel-inverted interferometer density profile after pellet injection In ohmic discharge. FTU pulse № 25 255 (reprinted from [13]): — 67; — 8; — 0.4 ms; — pre pellet

One of the most important characteristics of the ohmic regime with pellets is the density peaking as is shown in Fig. 5. The density peaking improves by a substantial factor after the pellet injection.

A feature of high field machines is the dependence of the density limit on the magnetic field. The Fig. 6 reports a comparison of the FTU data ordered vs the value of $I_p/(\pi a^2)$ (Greenwald density) and vs the toroidal magnetic field on axis B_T: showing that it's the latter the order parameter for the central density limit. The central density limit is therefore given by the following scaling law [23] $n_{e\ new} = CB^{1.5}$, where C is a function of the safety factor.

Summary of the experimental evidences from high field tokamaks ALCATOR-C-MOD. Experiments on

Alcator-C-MOD confirmed that there is a critical density after which the LOC (Linear ohmic confinement) switches to saturated ohmic confiment (SOC) and the confinement time is seen to follow the τ_E ITER-89P scaling law [5]. Fig. 7 shows the SOC density (i.e. the critical transition density above which the ohmic confinement saturates) vs the major radius for various devices as reported in [5]: the density at the confinement saturation is decresing as $1/R$.

It has been demonstrated on Alcator-C-MOD that the transition to SOC happens at a fixed collisionality where

$$\nu^* = \frac{\text{collision frequency}}{\text{bounce frequency}} \approx \frac{qRZ_{\text{eff}} n_e A^{3/2}}{T^2} \quad [5],$$

validating the scaling $n_{e\,\text{SOC}} \approx \frac{1}{qR}$. These data are taken on Alcator-C-MOD at a toroidal magnetic field B_T = 5.2 T. In Fig. 8 the transition from LOC to SOC is reported in a density scan, together with the curves representing the neo-Alcator scaling (eq. 1) and the ITER-89P L-mode scaling.

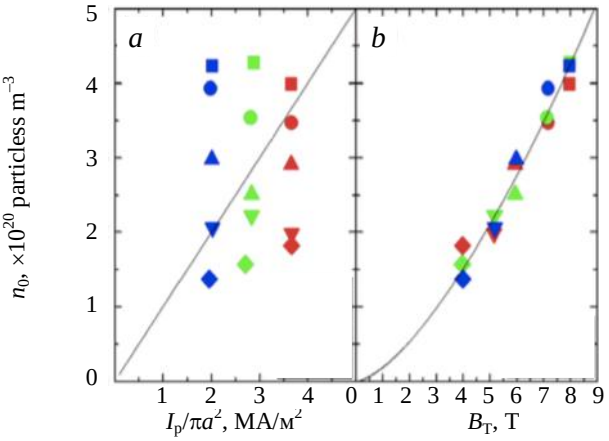

Fig. 6. Central line-averaged density at the disruption for the density limit versus the plasma current density for different BT (*a*) and versus BT for different Ip values (*b*). See boxes in the figure for the meaning of symbols and colours. The solid lines correspond to the Greenwald density limit n_G: ■ — 8; ● — 7.2; ▲ — 6; ▼ — 5.2; ◆ — 4 T (*a*) and to the new scaling law $n_{e\,\text{new}}$ (reprinted from [23]): ● — 900; — 700; — 500 kA (*b*)

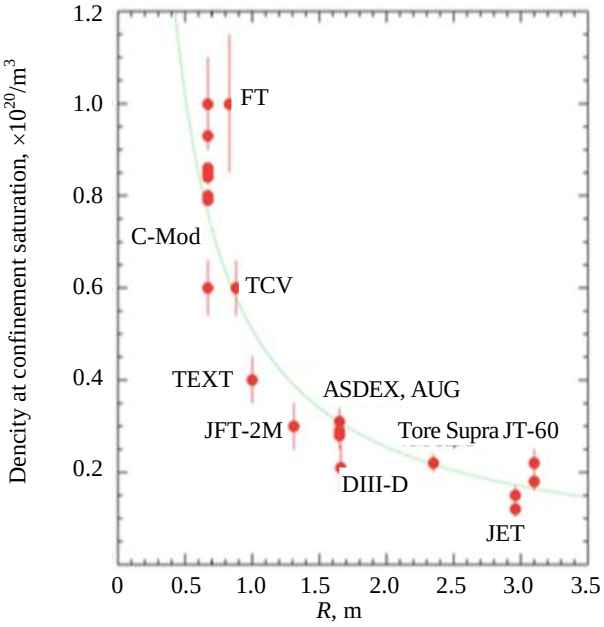

Fig. 7. The transition density from LOC to SOC as a function of major radius for different devices at fixed values of q (safety factor) in the interval q = 2.8—3.8. The solid curve represents $1/R$ dependence (reprinted from [5])

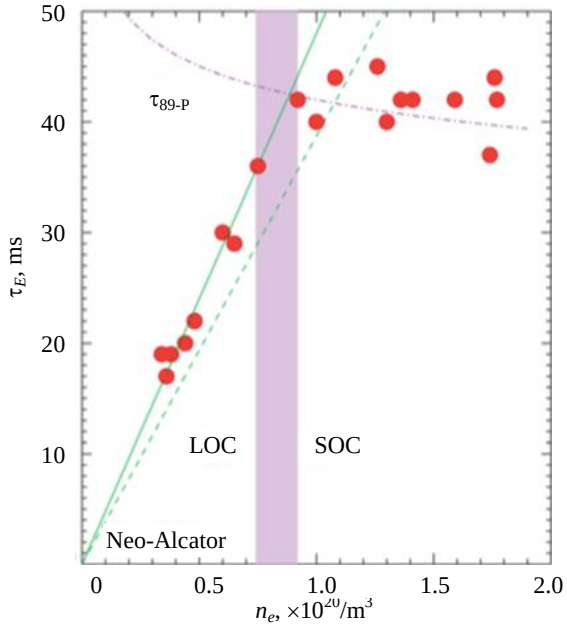

Fig. 8. The energy confinement time (from kinetic profiles) as a function of average electron density for a series of 5.2 T, 0.81 MA ohmic discharges. The shaded vertical bar indicates the boundary between the LOC and SOC regimes. The dashed line is the neo-Alcator scaling, the solid line is the best fit to the low density points, and the dash-dot line is the ITER-89P L-mode scaling. (reprinted from [5])

DESIGN CRITERIA FOR A MCF (MAGNETIC CONFINEMENT FUSION) NEUTRON SOURCE: SCALING LAWS FOR TOKAMAK FUSION REACTOR PLASMAS

The criteria determining the parameters for a fusion neutron source can be set by conditions useful to derive scaling laws specific for fusion reactors, where the alpha particle power is an important quantity entering the physics of the system. We can define a set of conditions useful for determining the working parameters of a fusion reactor (FR) [22, 24]:

— FR1. $Q = Q_0$ fixed: the fusion gain factor Q is taken fixed to a defined value $Q = Q_0$;

— FR2. $\tau_{SD} = \Lambda_{SD}\tau_E(\Lambda_{SD} << 1)$, i.e. τ_{SD} slowing down time of alpha particles $<<\tau_E$ energy confinement time, Λ_{SD} is a numerical constant);

— FR3. $P_0 = \Lambda_{LH} P_{LH}$ (P_α is the alpha power; P_{LH} here is the power threshold for entering the H-mode (High Confinement mode) and the formula used is the Martin scaling [15]; Λ_{LH} is a numerical constant). Here two possibilities are considered in relation to the value of the numerical constant Λ_{LH};

— FR3.1. $\Lambda_{LH} < 1$, the alpha heating can be relatively low and not sufficient to keep the plasma in H-mode;

— FR3.2. $\Lambda_{LH} > 1.5$, the alpha heating can be sufficient to keep the plasma in H-mode.

If we use the L-mode confinement time scaling [25] for defining the functional dependences on the plasma parameters in the previous condition FR2, We find that the scaling parameter linking equivalent fusion plasmas is:

$$S_{FR}\left[\text{L-mode}\right] = f(\Lambda_{SD}, \Lambda_{LH}, f_\alpha, M_{eff}) R B^{5/2} A^{-3/4} Q_0^{-0.7}, \tag{2}$$

where R is the tokamak major radius; B the toroidal magnetic field on axis; the aspect ratio of the tokamak ($A = R/a$); Q_0 is the fusion gain factor, which here is supposed not high. The function $f(\Lambda_{SD}, \Lambda_{LH}, f_\alpha, M_{eff})$ depends on the numerical constants Λ_{SD}, Λ_{LH}, M_{eff} (plasma effective ion mass) and f_α (the plasma diluition).

The possibility of having enough alpha particles power to keep the plasma in H-mode can be also considered: therefore in condition FR2 the ITER H-mode IPB-98 (y, 2) scaling law of confinement time [25] must be used and $\Lambda_{LH} > 1$ is implicit in condition FR3. The scaling parameter for these fusion plasmas is:

$$S_{FR}\left[\text{H-mode}\right] = f(\Lambda_{SD}, \Lambda_{LH}, f_\alpha, M_{eff}) R B^{4/3} A^{-1} Q_0^{1/3}. \tag{3}$$

The scaling law was used in [22] for the analysis of medium size tokamaks parameters.

In this paper Spherical Tokamaks (ST) are considered as well, as candidate neutron sources: in this case, in the condition FR2, the confinement time scaling typical of the ST [19] will be used together with the condition $\Lambda_{LH} > 1.5$ and the same scaling law for the H-mode power threshold. The same calculations (as in the previous cases) can be done and the result is the scaling parameter S_{ST} (NSTX scaling) or ST:

$$S_{ST}[\text{NSTX scaling}] = C_{ST} R_{ST}^{-1} Q_0^{0.61} B^{-1.13} A^{1.59} M_{eff}^{0.22} q^{0.4};$$

$$C_{ST} = \left(\frac{\Lambda_{SD}}{A_{SD}}\right)^{-0.036} \left(\frac{\Lambda_{LH} A_{lh}}{f_\alpha}\right)^{0.24}, \tag{4}$$

where A_{SD}, A_{lh} are numerical constants related to the slowing down time, and to the L—H-transition scaling law. The following meaning can be associated to the eqs. 2, 3 and 4: the value of S_{FR} and S_{ST} define families of equivalent fusion plasmas in terms of confinement and fusion gain. In equations 2, 3 and 4, a DT-plasma is considered. Strictly speaking the formula (4) is derived using the NSTX confinement scaling law, which is valid only for $A = 1.4$ and the safety factor $q = q$ NSTX, then we can use the final form of the ST scaling parameter:

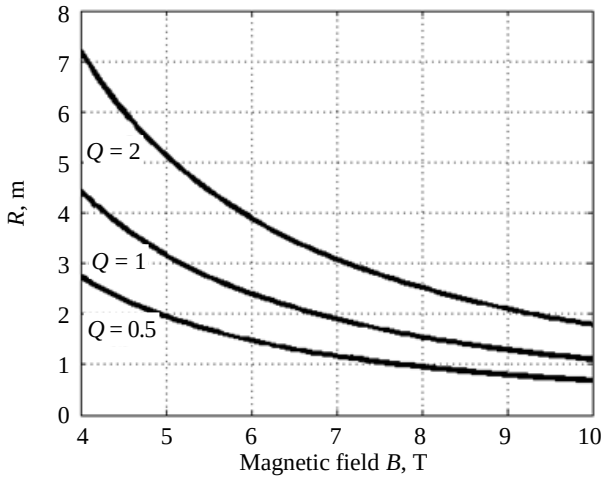

Fig. 9. Major radius vs magnetic field on axis at gain factors $Q_0 = 0.5$, 1, 2, for devices with aspect ratio $A = 2.5$, $q_{cyl} = 3.47$

$$S_{ST}[\text{NSTX scaling}] = C'_{ST} R_{ST}^{-1} Q_0^{0.61} B^{-1.13};$$

$$C'_{ST} = \left(\frac{\Lambda_{SD}}{A_{SD}}\right)^{-0.036} \left(\frac{\Lambda_{th} A_{lh}}{f_a}\right)^{0.24} \left[A^{1.59} M^{0.22} q^{0.4}\right]_{NSTX}. \tag{5}$$

Determination of the parameters of a high field tokamak as a fusion neutron source. Using the above scaling relations, we can evaluate the design characteristics of a high field tokamak as a neutron source. Two design scenarios are considered — a medium aspect ratio machine with $A = 2.5$ and a low aspect ratio machine with $A < 1.8$.

The Fig. 9 shows a plot of the major radius versus the magnetic field on axis at gain factors $Q_0 = 0.5$, 1,2, for aspect ratio $A = 2.5$ and $q_{cyl} = 3.47$, corresponding to the family of tokamaks having the scaling factor of eq. 2. and following the L-mode ITER-97P confinement scaling.

From Fig. 9 the following parameters of devices can be deduced: $Q = 1$, $B = 8$ T, $R = 1.5$ m, $A = 2.5$, $q_{cyl} = 3.47$; $Q = 2$, $B = 8$ T, $R = 2.5$ m, $A = 2.5$, $q_{cyl} = 3.47$.

To check the validity of the scalings, the SPECTRE [26] code was used to generate a self consistent design for the $Q = 1$ device, working at $B = 8$ T, consistent with $P_{fus} = 8$ MW. The plasma parameters of such a device where a neutron yield of the order of 10^{18} n/s is reported:

Parameters	Value
H_{97} . . .	1.2
A_{SP} . . .	2.5
Q . . .	1
R_0, m . . .	1.66
a, m . . .	0.66
Kappa . . .	1.8
I_p, MA . . .	7.26
B_T, T	8.0
P_{fus}, MW . . .	8.0
n_{avg}, 10^{20} m^{-3} . . .	1.43
$<T_e>$, keV . . .	3.9
τ_E, s . . .	0.56
P_{OH}, MW . . .	3.95
q_{95} . . .	4.45
Z_{eff} . . .	1.7
β_P . . .	0.22
W_{therm}, MJ . . .	6.64
Neutron yield, s^{-1} . . .	2.84×10^{18}

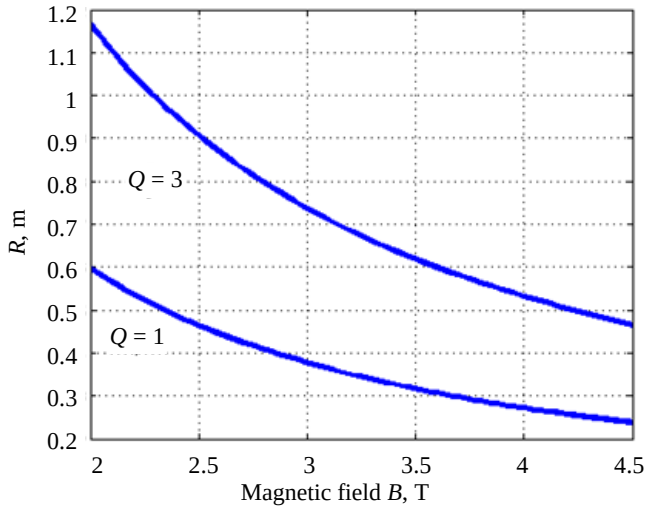

Fig. 10. Major radius vs magnetic field B on axis for spherical tokamaks with aspect ratio $A = 1.8$

Plasma parameters evaluated by SPECTRE system code for a $Q = 1$ device, $B = 8$ T and consistent with the calculations reported in Fig. 9.

Fig.10 reports the major radius vs magnetic field, using the scaling (5) for ST. Two sets of parameters can be deduced from Fig. 10: $A = 1.8$, $B = 3$ T, $Q = 1$, $R = 0.4$ m; $A = 1.8$, $B = 3$ T, $Q = 3$, $R = 0.75$ m.

The analysis made using the SPECTRE system code has been extended also to the ST, whose parameters can be deduced from Fig. 10. SPECTRE system code evaluation of a $Q = 1.6$, $A = 1.6$ and $Q = 3$, $A = 1.8$ ST device:

H_{98} . . .	3.3	2.9
A_{SP} . . .	1.6	1.8
Q . . .	1.6	3.0
R_0, m . . .	0.4	0.75
a, m . . .	0.25	0.416
Kappa . . .	2.8	2.8
I_p, MA . . .	2.94	4.5
B_T, T . . .	3.0	3.0
P_{fus}, MW . . .	16.25	30.1
n_{avg}, 10^{20} m^{-3}, . . .	4.18	2.15
$<T_e>$, keV . . .	7.8	9.9
τ_E, s . . .	0.17	0.47
q_{95} . . .	8.8	7.0
Z_{eff} . . .	1.73	1.73
β_{th}, % . . .	29	19.2
β_N . . .	7.45	5.33
W_{therm}, MJ . . .	2.04	6.96
Neutron yield, s^{-1} . . .	5.78×10^{18}	1.1×10^{19}

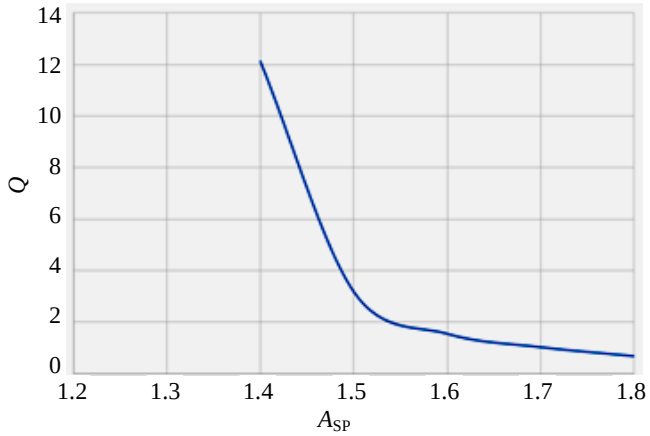

Fig. 11. System code results of the gain factor Q vs aspect ratio A_{SP} for a ST with R = 0.4 m, heating power $P_{heat} = 10$ MW, HH = 3.3 (the confinement factor with respect to the ITER IPB-98 (y 2) confinement scaling law), and magnetic field on axis $B = 3$ T

The parameters of a $Q = 3$ ST device working at aspect ratio $A = 1.8$ evaluated by the SPECTRE system code, and consistent with the results shown in Fig. 10.

A study has been carried out using the SPECTRE system code [26] related to the maximun gain factor achievable by a ST with $R = 0.4$ m, heating power $P_{heat} = 10$ MW, HH = 3.3 (the confinement factor with respect to the ITER IPB-98 (y 2) confinement scaling law), and magnetic field on axis $B = 3$ T, varying the aspect ratio. The results are shown in Fig. 11: the gain factor is a critical function of the aspect ratio: in the region of $A_{SP} = 1.4$—1.5 the gain factor can change by a substantial factor (5X).

TRL (TECHNOLOGY READINESS LEVEL) ASSESSMENTS FOR FUSION FISSION HYBRID REACTOR APPLICATION

In the context of FFH reactors, the following type of machine is in consideration:

— fusion gain Q ~ 2—3 machine with long pulses (say >3 hrs)/steady state, DT-plasma P_{DT} ~ 20—100 MW, $P_{in} \geq 10$—30 MW;

— low level of probability of disruptions: plasma parameters chosen to be away from strong MHD and density limits (for example with $\beta_N < 2.5$ for $A \geq 2.5$, $n/n_{Gr} < 0.8$);

— power on the divertor definitely lower than 5 MW/m^2: in this case the problem of the divertor is easier;

— a blanket for tritium breeding with power gain and neutron multiplication from fission;

— a machine with high reliability, working continuously;

— all maintenance by remote handling;

— modularity (facilitating rapid interventions on the divertor);

— few and simple diagnostics (the acceptable level of complexity of the diagnostics and controls depends on the plasma scenario and on the physics model).

The meanings of the different technology readiness levels are as described in [27].

The Table 3 (for devices with pulse length of 100 s) and Table 4 for devices with pulse length of 1000 s show TRL for the main subsystems of a tokamak neutron source for FFH: it seems that only ECRH (electron cyclotron resonant heating) systems are at a level of engineering maturity for the insertion in a FFH, while the other main systems need to be demonstrated in a neutron flux environment Although the most important developments differ slightly, the steps in TRL are not fine enough to distinguish the 100 and 1000 s FFH concepts.

T a b l e 3. **Technology Readiness Level for prototype with 100-second pulses**

Subsystem	TRL 100 s	Comments
Superconducting magnets	4	Not demonstrated in a neutron flux environment.
NBI (100 keV)	4	Need to demonstrate immunity to gamma and neutron effects (e.g. grid flash-over due to the ionising radiation or grid insulation degeneration).
ECRH (1 MW gyrotron)	6	The gyrotrons are not in any radiation field and steady state operation has been demonstrated at the developer's works, for hours if not months, but only on test-beds.
ICRH (1 MW)	4	As NBI but for antenna operation; also parasitic currents may inject antenna material into the plasma.

T a b l e 4. **Technology Readiness Level for prototype with 1000-second pulses**

Subsystem	TRL 1000 s	Comments
Superconducting magnets	4	Not demonstrated in accumulated neutron fluence.
NBI (100 keV)	4	Need to show long-term reliability and immunity to large neutron fluence (e.g. grid distortion).
ECRH (1 MW gyrotron)	6	As NBI but for antenna damage.
ICRH (1 MW)	4	As NBI but for antenna damage.

Table 5 shows the TRL for the plasma scenarios: here only the H-mode demonstrated on JET DTE1 at $Q < 1$ can be considered for FFH reactor designs. The other scenarios need a demonstration at least at low power.

T a b l e 5. **Technology Readiness Level for possible operational scenarios**

Scenario	TRL	Comments
L-mode and H-mode	6	OK in JET at Q ~ 0.6, needs demonstration at Q ~ 2
Hybrid mode	4	Needs demonstration in relevant $Q \approx 1$ environment – possibly JET DTE2
Advanced mode	3	To be demonstrated in a near steady-state machine

CONCLUSIONS

The recent advances of the superconductor technology has brought the attention to the possible feasibility of very compact fusion reactors at high field. Along this line of research in this paper , tokamak neutron sources working with a magnetic field $B \approx 8$ T, and aspect ratio $A = R/a = 2.5$ are considered. The paper summarizes the main experimental evidences deduced from the operation of the high field tokamaks of the Alcator family (Alcator-A, Alcator-C and Alcator-C-MOD) and the Frascati tokamaks (FT) and FTU (Frascati tokamak upgrade): ohmic operation or operation in L-mode (see ITER Phys Basis [25]) is considered. A scaling law for fusion reactors working with D:T mixture in L-mode is derived following the analysis of [22, 24] and a $Q \approx 1$

fusion neutron source with major radius $R \approx 1.5$ m at $B = 8$ T is determined. The ST are also considered in the analysis of fusion neutron sources. The scaling law of confinement derived from the operations of NSTX, START and MAST [16—19] spherical tokamaks is used in the scheme for the derivation of scaling law for ST reactors. In this case the parameters for a $Q = 1$, aspect ratio $A = 1.8$, neutron source are $B = 2$ T and $R = 0.8$ m. The TRL of tokamak subsystems is analyzed, where the TRL classification reported in [27] is adopted. A TRL ≈ 4 can be associated (in average) to the subsystems of a tokamak neutron source: this means that the basic validation in laboratory has been carried out for the main subsystems. The TRL ≈ 6 can be associated to the plasma scenarios L-mode and H-mode: this means that the scenarios must still be validated in $Q > 1$ plasma environment. The results reported are based only on theoretical physics analysis, the engineering constraints (such as the shieldings which must be included in the design of tokamak devices) are not considered in the present analysis.

REFERENCES

1. **Creely A.J. et al.** Overview of the SPARC tokamak. — J. Plasma Phys., 2020, vol. 86, p. 865860502.
2. **Whyte D.** Small, modular and economically attractive fusion enabled by high temperature superconductors. — Phil. Trans. R. Soc. A377, p. 20180354.
3. **Coppi B. et al.** Optimal regimes for ignition and the Ignitor project. — Nucl. Fusion, 2001, vol. 41, p. 1253.
4. **Sorbom B.N. et al.** ARC: a compact high field fusion nuclear science facility and demonstration power plant with demountable magnets. — Fus. Eng. Des., 2015, vol. 100, p. 378.
5. **Rice J.E. et al.** Ohmic energy confinement saturation and core toroidal rotation reversal in Alcator-C-MOD plasmas. — Phys. Plasmas, 2012, vol. 19, p. 056106.
6. **Rice J.E. et al.** Understanding LOC/SOC phenomenology in tokamaks. — Nucl. Fusion, 2020, vol. 60, p. 105001.
7. **Greenwald M. et al.** Energy confinement of high-density pellet-fuelled plasmas in the Alcator C Tokamak. — Phys. Rev. Lett., 1984, vol. 53, p. 352.
8. **Parker R.R. et al.** Progress in tokamak research at MIT. — Nucl. Fusion, 1985, vol. 25, p. 1127.
9. **Wolfe S.M. et al.** Effect of pellet fuelling on energy transport in ohmically heated Alcator C plasmas. — Nucl. Fusion, 1986, vol. 26, p. 329.
10. **De Marco et al.** High magnetic field tokamaks. — Nucl. Fusion, 1986, vol. 26, p. 1193.
11. **Alladio F. et al.** Energy confinement at high density in FT tokamak. — Nucl. Fusion, 1982, vol. 22, p. 479.
12. **Bracco G., Buratti P., Orsitto F., Santi D.** Energy confinement scaling laws for FT ohmic plasmas. — In: 17th EPS Conference on Controlled Fusion and Plasma Heating. Amsterdam, 25—29 June 1990, vol. 14B, p. 118; and ENEA Report RT/NUCL/90/04.
13. **Fusion** Science and Technology Special Issue on Frascati Tokamak Upgrade (FTU) 2004, vol. 45, № 3: Chapter 2. **Gormezano C. et al.** Highlight of the physics studies in the FTU, p. 203; Chapter 4. **Frigione D. et al.** High Density regimes, p. 339; Chapter 6. **Esposito B. et al.** Transport studies, p. 370.
14. **Esposito B. et al.** Transport analysis of ohmic, L-mode and improved confinement discharges in FTU. — Plasma Phys. Controlled Fusion, 2004, vol. 46, p. 1793.
15. **Martin Y.R. et al.** Power requirements for accessing the H-mode in ITER. — J. of Physics Conf. Series, 2008, vol. 123, p. 01233.
16. **Menard J.E. et al.** Overview of the physics and engineering design of NSTX. — Nucl. Fusion, 2012, vol. 52, p. 083015, and **Menard J.E. et al.** Overview of NSTX upgrade initial results and modelling highlights. — Nucl. Fusion, 2017, vol. 57, p. 102006.
17. **Gryaznevich M. et al.** Overview and status of construction of ST40. — Fus. Eng. Des., 2017, vol. 123, p. 177.
18. **Chuyanov V.A., Gryaznevich, M.P.** Modular fusion power plant. — Fus. Eng. Des., 2017, vol. 122, p. 238.
19. **Buxton P.F. et al.** On the energy confinement time in spherical tokamaks: implications for the design of pilot plants and fusion reactors. — Plasma Phys. Contr. Fusion, 2019, vol. 61, p. 035008.
20. **Snipes J. et al.** Characteristics of high-confinement modes in Alcator-C-MOD. — Phys. Plasmas, 1996, vol. 3, p. 1992.
21. **Ma. Y. et al.** Scaling of H-mode threshold power and L—H edge conditions with favourable ion grad-B frift in Alcator-C-MOD tokamak. — Nucl. Fusion, 2012, vol. 52, p. 023010.
22. **Orsitto F.P., Todd T.N.** Tokamaks as neutron sources for Fusion-Fission hybrid reactors: analysis of design parameters and technology readiness levels. — In: Proceedings FUNFI3 Conference 2019; https://www.enea.it/en/publications/abstract/funfi3-international-conference-on-fussion-fission.
23. **Pucella G. et al.** Dependence of the density limit on the toroidal magnetic field on FTU. — Nucl. Fusion, 2013, vol. 53, p. 023007.
24. **Romanelli M. et al.** On the optimal choice of the dimensionless paramenters of burning plasma physics experiments. — In: 28th EPS Conference on Contr. Fusion and Plasma Phys., Funchal 18—22 june 2001, ECA vol. 25 p. 697.
25. **ITER** Physics basis. Chapter 2. Plasma confinement and transport. — Nucl. Fusion, 1999, vol. 39, p. 2204 (formula (21) for H-mode energy confinement time), and p. 2205 (formula (25) for L-mode).
26. **Menon V.** Physics Design and Analysis code SPECTRE for Tokamak based fusion reactors. — 25th IAEA FEC 2014.
27. **Orsitto F.P. et al.** Diagnostics and controls for steady state and pulsed tokamak DEMO. — Nucl. Fusion, 2016, vol. 56, p. 026009.
28. **Blackwell B. et.al.** Energy and Impurity Transport in the Alcator C Tokamak. IAEA-CN-41/I-3. Plasma Physics and Controlled Nuclear Fusion Research. IAEA FEC Conference Baltimora, 1982; see also **C. Gao et al.** Non-local heat transport in Alcator-C-MOD ohmic L-mode plasmas. — Nucl. Fusion, 2014, vol. 54, p. 083025.

29. **Gormezano C.** Highlights of the physics studies in the FTU. — Fusion Science and Technology, 2004, vol. 45.
30. **Greenwald M. et al.** Energy confinement of high-density pellet-fueled plasmas in the Alcator C Tokamak. — Physical Review letters, 1984, vol. 53, № 4.

AUTHORS

Francesco Paolo Orsitto; ENEA Department for Fusion and Nuclear safety, C.R. Frascati, E. Fermi 45, 00044 Frascati, Italy, francesco.orsitto@enea.it

M. Romanelli; Tokamak Energy Ltd., 173 Brook Drive, Milton Park, Oxfordshire, OX14 4SD, United Kingdom

M. Vinay; Institute of Plasma Research, Gandinaghar, Gujarat, India

Received 15 January 2021
Revised 16 March 2021
Accepted 25 March 2021
Problems of Atomic Science and Technology
Ser. Thermonuclear Fusion, 2021, vol. 44, issue 2, pp. 47—56